Theory of Carbon Nanocones: Mechanical Chiral Inversion of a Micron-Scale Three-Dimensional Object

Stephen P. Jordan and Vincent H. Crespi
Department of Physics and Materials Research Institute, Pennsylvania State University, University Park, Pennsylvania 16802-6300, USA
(Received 13 July 2004; published 15 December 2004)

Graphene cones have two degenerate configurations: their original shape and its inverse. When the apex is depressed by an external probe, the simulated mechanical response is highly nonlinear, with a broad constant-force mode appearing after a short initial Hooke's law regime. For chiral cones, the final state is an atomically exact chiral invert of the original system. If the local reflection symmetry of the graphene sheet is broken by the chemisorption of just five hydrogen atoms to the apex, then the maximal yield strength of the cone increases by ~40%. The high symmetry of the conical geometry can concentrate micron-scale mechanical work with atomic precision, providing a way to activate specific chemical bonds.

DOI: 10.1103/PhysRevLett.93.255504 PACS numbers: 62.25.+g, 61.46.+w

Removing a 60° wedge from a graphene sheet and joining the edges produces a cone with a single pentagonal defect at the apex. Removing additional wedges introduces more such defects and reduces the opening angle. A cone with six pentagons has an opening angle of zero and is just a nanotube with one open end. Ge and Sattler [1] originally discovered carbon nanocones in 1994, and Krishnan *et al.* [2] have subsequently synthesized cones with all five opening angles. The low-energy electronic states of graphene nanocones are profoundly altered by geometrical phases associated with the apical pentagon(s), which can intertwine the graphenic Fermi points, create interference without diffraction, and introduce singularities into the local density of states [3,4]. Shenderova *et al.* [5] used molecular dynamics simulations to manipulate nanocones into metastable states. Here, we show how the high symmetry of the conical structure and the local reflection symmetry of a graphene sheet combine to produce unusual mechanical properties under compression by a probe tip.

Initially, a graphene cone responds as a Hooke's law spring. However, as a small threshold force is exceeded, the mechanical response abruptly transitions to a constant-force mode where elastic energy is stored in the fold that divides the upward and downward facing portions of the cone. Further compression eventually completes the inversion, yielding a final state that is an exact chiral invert of the original system. Unlike plastic deformation, the quadratic-linear transition is reversible with no residual deformation. If just five hydrogen atoms are bonded to the apical pentagon, the yield strength increases by 40%.

We study cones with from one to three pentagonal defects at the apex arranged as shown in Fig. 1. The outer edge of the cone (trimmed to be roughly circular) is capped with hydrogen. Chemical bonding within the cone is modeled with the Tersoff-Brenner potential [6], which can describe the essential physics [7]. A plane supports the cone from below and a spherical indenter presses down on its apex, as shown in Fig. 2. The sphere and plane are continuous media which interact with the cone via a Lennard-Jones interaction. This simple form helps to isolate the mechanical response of the cone itself and is reasonable in light of the low reactivity of a graphene basal plane. The Lennard-Jones parameters are $\sigma_6^6 = 20$ eV Å^6 and $\sigma_{12}^{12} = 2.48 \times 10^4$ eV Å^{12} [8].

Since an experimental probe is slow compared to atomic-scale motions, we use a quasistatic approximation. The spherical indenter approaches the cone in small increments with a relaxation of the atomic coordinates after each step, using the Polak-Ribiere variant of the conjugate gradient method. Before each relaxation, small random perturbations of a few hundredths of an Angstrom are applied to each atom to break symmetry. For the two and three pentagon cases the cone's center of mass was fixed to prevent it from sliding sideways out from underneath the indenter. A roughened substrate or indenter could have this effect.

When the indenter first touches the cone, the energy increases quadratically; this Hooke's law regime is labeled I in Fig. 3. The cone soon deviates from the quadratic behavior as the dent gradually deforms to better match the shape of the indenter. In region II, the dent does

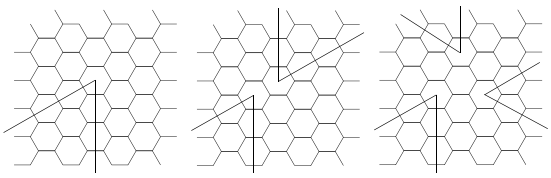

FIG. 1. Removing these wedges and joining the free edges to create pentagonal defects produces the apices of the cones studied here.

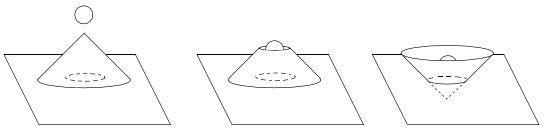

FIG. 2. Schematic of a typical simulation. On the right, the apex pokes through a circular hole in the substrate.

not yet fully accommodate the indenter, so the indenter pushes on its rim, producing a gradual softening without a simple functional form. The partially dented region is still relatively stiff, so some internal energy is stored near the base of the cone, as shown in the first frame of Fig. 3.

Next, the cone abruptly buckles, producing a well-defined circular fold at the transition between upward and downward sloping sidewalls, as shown in the second frame of Fig. 3. The discontinuity in the cone's internal energy is larger than the jump in the total energy (including the interactions with the indenter and the substrate), since compressive stress at the base of the cone is relieved. This event marks the beginning of the constant-force regime. In region III, the circular fold dominates the energetics. This fold has a nearly constant energy per unit length. Since the circumference of the fold is linear in the displacement of the indenter, the system acts as a nearly constant-force spring over a wide range, with a force of 0.7 eV/Å, or 1.1 nanoNewtons. When the expanding fold reaches the base of the cone, it escapes through the cone's edge and the structure is fully inverted, with a second, much larger discontinuity in total energy (a "snap through"). The total energy of the fully inverted cone slightly exceeds the initial energy because the orientation of the upside-down cone relative to the indenter and substrate (see Fig. 2) changes the Lennard-Jones interaction energy between these subunits.

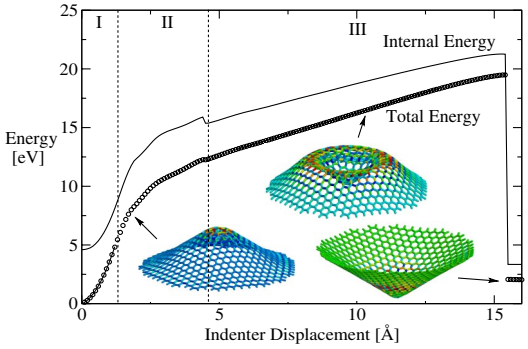

FIG. 3 (color online). Inversion of a single-pentagon nanocone pressed by a spherical indenter. The internal energy includes only the Tersoff-Brenner contributions, while the total energy includes the interactions with the indenter and substrate. The quadratic fit in region I yields a spring constant of 2.6 eV/Å^2. The linear fit in region III yields a nearly constant force of 0.7 eV/Å. The indenter and cone have radii of 5 and 24 Å, respectively. The substrate is a flat plane with a circular hole of radius 15 Å directly below the cone's apex.

This highly nonlinear and reversible mechanical response can be ascribed to the high symmetry structure: the degeneracy of upward and downward sloping sidewalls allows mechanical energy to be concentrated in the transition region between these two nearly equivalent local-equilibrium states. In the linear elastic response of a normal material, every atom stores some fraction of the elastic energy, and as the deformation increases the elastic energy density in any given region scales quadratically with displacement. In contrast, for the constant-force regime of the graphene cone, the energy density in the deformed region (i.e., the fold) *remains constant* while the *number* of elastically deformed atoms (i.e., the circumference of the fold) increases *linearly* (not quadratically) with the displacement. This mechanism is distinct from the constant-force mode of a buckled nanotube [9], which follows the theory of buckled beams [10].

The plane underneath the cone has a circular hole located just below the cone's apex. This geometry simplifies the analysis by eliminating contact between the apex and the underlying plane during the inversion. In an experiment, a similar effect could result from surface roughness. Using a solid plane truncates region III and can prevent the cone's complete inversion.

A cone with two pentagons, with an opening angle of 84°, responds similarly, with a slightly different behavior in region II, where the increased rigidity of the two-pentagon cap produces a larger deformation near the base and the cone takes on an elliptical cross section aligned with the axis connecting the pentagons (see Fig. 4). At the transition to region III, the cone regains a nearly circular cross section and again behaves as a constant-force spring, with a force 1.2 times larger than that for the single-pentagon cone. A nanocone with three pentagons, which has an opening angle of 60°, fails to invert when pressed by the 5 Å indenter. Rather, the tip of the cone bends out of the path of the indenter.

If the cone contains structural imperfections which are reflection-symmetric about the local sp^2 plane, such as

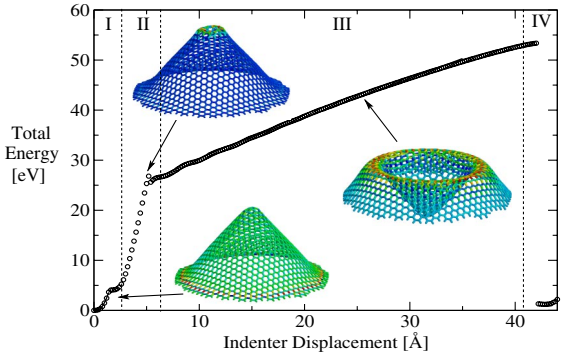

FIG. 4 (color online). Inversion of a two-pentagon nanocone of radius 30 Å, with an indenter of radius 4 Å. The linear fit in region III yields a force of 0.8 eV/Å, and the quadratic fit in region I yields a spring constant of 2.9 eV/Å^2.

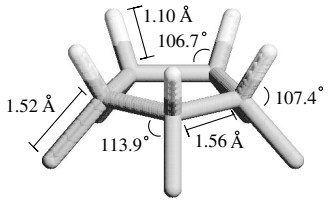

FIG. 5. The relaxed geometry of the apex of a nanocone with hydrogen atoms bonded to the pentagonal carbon.

boron or nitrogen substitution, carbon vacancies or a ragged external edge (or for a two-pentagon cone, just one of these imperfections in a low-symmetry position), then it is a chiral object. After inversion, the chirality reverses, with atomic-scale perfection, even for cones of micron size. This is like turning a glove inside out, except that the inner and outer surfaces of a graphene cone are indistinguishable, so the chiral inversion of the nanocone is perfect. It is also similar to the resonant inversion of ammonia, but in a much larger and chiral object, possibly as big as a small integrated circuit. Normally, a true chiral inversion of a large-scale three-dimensional object without breaking and reforming bonds is impossible without going into the fourth dimension. Whether this unique property of the graphene cone could be used to create switchable optical activity or mesoscopic tests of fundamental symmetries remains to be seen.

Chemical modifications which break the local reflection symmetry of the graphene sheet can profoundly change the mechanical response. Since chemical reactivity increases in highly curved regions of a graphene sheet, one could selectively bond ligands to the carbon atoms in the pentagonal ring(s) at the apex of the cone. Such functionalization creates sp^3-bonded carbon atoms and thereby breaks the reflection symmetry of the sp^2-bonded plane. As an example, we attach five hydrogen atoms, one to each carbon atom in the pentagon at the apex, as in Fig. 5. Figure 6 shows that the addition of just these five

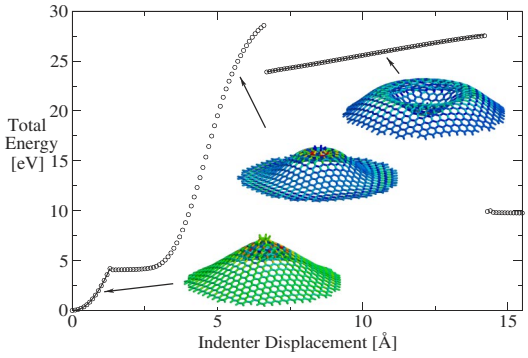

FIG. 6 (color online). The energetics of inversion for a single-pentagon cone with five hydrogen atoms bonded to the apex. The radius of the cone is 24 Å. The radius of the indenter is 5 Å. The quadratic fit yields a spring constant of 2.7 eV/Å^2, and the linear fit yields a force of 0.5 eV/Å.

hydrogen atoms to a cone with thousands of carbon atoms increases the yield strength by 40% and decreases the constant force by 30%. Complete inversion is now frustrated and the apical pentagon remains upright even after the rest of the cone has inverted, as shown in Fig. 7. The local bonding geometry is very unusual and highly strained. Since the structure is otherwise up-down symmetric, the hydrogen atoms have in effect been transferred to the underside of the cone; chemically, it would have been impossible to have attached them to this side directly.

The excess internal energy of this frustrated-inverted state (7.0 eV within the Tersoff-Brenner approximation) destabilizes the bound hydrogens by roughly 1.4 eV each, reducing their average binding energy to the cone from 3.2 to 1.8 eV relative to free H. Other ligands X should behave similarly, so this procedure provides a general mechanism to activate a C—X bond by about 1 eV. In some cases, this may make the bonds metastable with respect to the formation of detached species such as H_2. The frustrated-inverted structure is locally stable, but a sufficiently large perturbation (e.g., a random 0.2 Å shift in the position of each carbon atom), enables the structure to revert to the original upright configuration, if the indenter is removed.

The high symmetry of the cone concentrates mechanical energy in a region much smaller than the dimension of the external probe tip. (A scanning tunneling microscope, in contrast, depends on an atomic-scale asperity for atomic resolution.) For example, in the highly strained frustrated-inverted state, the ring of sp^2 atoms immediately surrounding the pentagon is highly distorted and therefore highly reactive, so it should be possible to attach additional ligands to these atoms, post inversion. If the cone is then pushed back the other way, one could iterate the process to produce concentric rings of sp^3 bonded carbon atoms within a graphene sheet, each ring with a different ligand attached, hanging from alternate sides of the sheet. It is well known how to create controlled atomic-scale variations in composition *perpendicular* to many surfaces through sequential deposition. The process described above provides a means to create atomic-scale patterns of controlled composition *parallel* to the surface of a carbon layer.

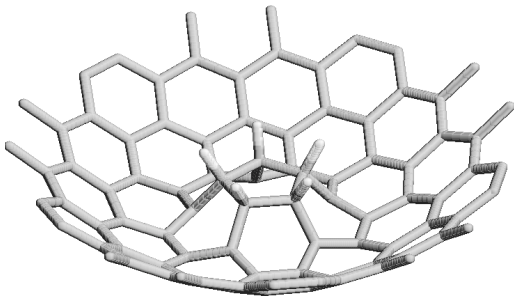

FIG. 7. The hydrogenated apex after inversion.

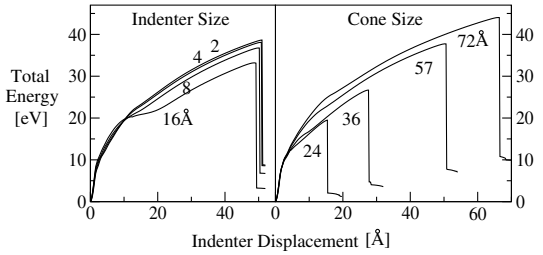

FIG. 8. Inversion of a cone of 57 Å radius as the indenter radius varies from 2 to 16 Å. Inversion of cones with radii from 24 to 72 Å for an indenter radius of 5 Å.

These phenomena are relatively generic and do not depend sensitively on the indenter radius or cone size. For example, Fig. 8 shows the inversion of a 57 Å radius nanocone for indenters with radii from 2 to 16 Å. The slope in the constant-force regime varies by only 7% as the radius varies from 2 to 16 Å. For a 32 Å indenter, the indenter approaches the size of the cone itself and the system shows a more idiosyncratic response. Similarly, cones with radius from 24 to 72 Å show similar elastic response, as shown in Fig. 8. We anticipate that multilayered unfunctionalized cones will show generally similar behavior, with scaled forces.

For the bare cones, if the small symmetry-breaking randomization of coordinates at each simulation step is omitted, similar behavior is also seen, except that a two-pentagon cone failed to invert in the absence of randomization when pressed with an indenter of radius 8 Å, instead bending out of the path of the indenter, as in the three pentagon case. For the functionalized cones, the greater apical stiffness occasionally favors an edge-nucleated inversion, where the fold initially appears at the base of the cone and moves upward (the final state, however, remains the same). All but one simulation of functionalized cones with randomization were center nucleated; this buckling mode is shown in Fig. 6. The exception occurred with an indenter radius of 16 Å in a cone of radius 24 Å. Without randomization, edge-nucleated buckling occurred in two cases, with indenter/cone radii of 2/24 and 5/36 Å respectively. The cones with a functionalized apex appear to be near a boundary between edge and center-nucleated inversion, the path taken being sensitive to parameters. However, the final state and the eventual concentration of mechanical energy onto the apical bonds are independent of the path.

Shenderova *et al.* [5] reported metastable partially inverted states for carbon cones. If such a state were encountered during inversion, the cone might fail to restore to its initial state upon removal of the indenter. In our simulations, a nanocone subjected to an oscillating indenter displays some weak hysteresis but does not become stuck in an intermediate state. Possibly, the presence of a substrate and indenter prevent the nanocones from finding the metastable configurations, with the exception that the final state of a frustrated-inverted functionalized cone does appear to be metastable, at least at $T = 0$.

We thank A. Kolmogorov, P. E. Lammert, D. Stojkovic, and E. Mockensturm for helpful discussions. We acknowledge the National Science Foundation for financial support through DMR-0305035 and DMR-0213623

[1] M. Ge and K. Sattler, Chem. Phys. Lett. **220**, 192 (1994).
[2] A. Krishnan, E. Dujardin, M. Treacy, J. Hugdahl, S. Lynum, and T. Ebbesen, Nature (London) **388**, 451 (1997).
[3] K. Kobayashi, Phys. Rev. B **61**, 8496 (2000); S. Garaj, L. Thien-Nga, R. Gaal, K. T. L. Forro, K. Takahashi, F. Kokai, M. Yudasaka, and S. Iijima, Phys. Rev. B **62**, 17 115 (2000); J. Charlier and G. Rignanese, Phys. Rev. Lett. **86**, 5970 (2001); R. Tamura and M. Tsukada, Phys. Rev. B **49**, 7697 (1994); R. Tamura, K. Akagi, M. Tsukada, S. Itoh, and S. Ihara, Phys. Rev. B **56**, 1404 (1997); S. Berber, Y. Kwon, and D. Tománek, Phys. Rev. B **62**, 2291 (2000).
[4] P. E. Lammert and V. H. Crespi, Phys. Rev. Lett. **85**, 5190 (2000); Phys. Rev. B **69**, 035406 (2004).
[5] Inversion was first investigated by Shenderova *et al.*, who focused on metastable structures and field-emission applications [Nanotechnology **12**, 191 (2001)].
[6] D. W. Brenner, O. A. Shenderova, J. A. Harrison, S. J. Stuart, B. Ni, and S. B. Sinnott, J. Phys. Condens. Matter **14**, 783 (2002).
[7] The essential physics of inversion is the global conical symmetry, the local reflection symmetry of a graphene plane, and the stability of graphene under distortions perpendicular to the plane. A more accurate (and computationally intensive) treatment would show some quantitative changes, e.g., in the magnitude of the constant force or the competition between edge and center nucleation, without changing the main thrust of the results.
[8] L. Girifalco and R. Lad, J. Chem. Phys. **25**, 693 (1956).
[9] B. I. Yakobson, C. J. Brabec, and J. Bernholc, Phys. Rev. Lett. **76**, 2511 (1996).
[10] S. Timoshenko and J. Gere, *Theory of Elastic Stability* (McGraw-Hill, New York, 1961), 2nd ed.